Journal of Advanced Research in Fluid Mechanics and Thermal Sciences

Journal homepage:
https://semarakilmu.com.my/journals/index.php/fluid_mechanics_thermal_sciences/index
ISSN: 2289-7879

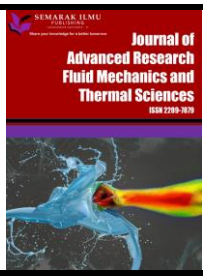

MHD Free Convection Boundary Layer Flow on a Horizontal Circular Cylinder in a Williamson Hybrid Ferrofluid with Viscous Dissipation

Marjan Mohd Daud[1], Muhammad Khairul Anuar Mohamed[1,*], Norhafizah Md Sarif[1], Huei Ruey Ong[2], Eddy Elfiano[3]

[1] Centre for Mathematical Sciences, Universiti Malaysia Pahang Al-Sultan Abdullah, Lebuh Persiaran Tun Khalil Yaakob, 26300 Kuantan, Pahang, Malaysia
[2] Faculty of Engineering & Technology, DRB-HICOM University of Automotive Malaysia, Peramu Jaya Industrial Area, 26607 Pekan, Pahang, Malaysia
[3] Department of Mechanical Engineering, Faculty of Engineering Universitas Islam Riau, 28284 Pekanbaru, Provinsi Riau, Indonesia

ARTICLE INFO

Article history:
Received 10 June 2024
Received in revised form 15 September 2024
Accepted 27 September 2024
Available online 20 October 2024

Keywords:
Hybrid ferrofluid; Keller-box method; Williamson fluid

ABSTRACT

The present research examined the flow of a horizontal circular cylinder immersed in a Williamson hybrid ferrofluid via free convection boundary layer flow. The fluid flow is modelled by means of governing partial differential equations that incorporate viscous dissipation and magnetohydrodynamic (MHD) effects. Prior to being converted into a more practical partial differential equation, these dimensional equations are reduced to a non-dimensional form by utilising appropriate dimensionless variables. The Keller-box approach is then used to solve these equations with fewer dependent variables numerically. Graphical representations are generated, and the impacts of different interested factors are analysed using MATLAB software. According to the results, the hybrid ferrofluid outperformed ferrofluid with the same particle volume fraction in terms of skin friction and convective heat transfer capabilities.

1. Introduction

The major objective of this research is to improve a fluid's thermal properties. Therefore, a better way to solve the issue is to submerge nano-sized particles in a certain base fluid. Notable progress has been made in the field of nanotechnology as a result of the trend. A particular type of nanofluids called ferrofluids is created when magnetic nanoparticles are suspended in a non-magnetic base fluid. This type of fluid can have its flow and heat transfer regulated when it is exposed to an external magnetic field and a temperature gradient [1]. Ferrofluid is designed to provide a spinning shaft seal for NASA spacecraft and liquid rocket fuel that might be attracted to a fuel pump in a weightless environment by the creation of a magnetic field, according to Stephen [2]. The term "ferrofluid" had already been developed, the procedure had been improved, more highly magnetic liquids had been created, and new types of carrier liquids had been found by then. Because of their special qualities

* *Corresponding author.*
E-mail address: mkhairulanuar@umpsa.edu.my

https://doi.org/10.37934/arfmts.122.2.121

and potential, ferrofluids have drawn a lot of attention from researchers studying their applications in the industrial and technical fields. For example, they are used to cool and lessen unwanted vibrations in loudspeakers' voice coil gaps. Ferrofluids have also been used to extract metal from ores because they take advantage of the change in fluid density that occurs when a magnetic field is applied. Besides, these fluids can also be employed in microfluidic and micromechanical systems. According to Oehlsen *et al.,* [3], ferrofluids have smaller particles, which extend the suspension duration and increase suspension stability. The most recently published research, addresses at heat, thermal radiation, and slip flow of ferrofluid towards various geometries, including boundary conditions for Newtonian heating, stretched surfaces, and stagnation [4-9].

In recent years, nanoparticles have been incorporated into cancer treatment drugs. These nanoparticles may freely move throughout the body through a blood vessel. It is known that the presence of gold in the blood did not bring damages to the body tissue. Hence, it is a very good particles to be used in cancer treatments. The cancer cells were eliminated by raising the temperature of the nanoparticles as stated in the earlier study [10]. Gold nanoparticles are the most important particles for shedding light, according to Alam *et al.,* [11]. Due to its structure, shape, low toxicity, and remarkable body compatibility, this issue has garnered a lot of attention from researchers lately. Based on studies by The Royal Institution [12], gold nanoparticle evaluation was conducted. Gold nanoparticles imbedded in various types of fluids, primarily blood, have been the focus of previous studies, which classified the fluid as a third-grade non-Newtonian fluid [13-15]. One particular category of fluid that conducts electricity is blood. The electro-magnetic force acting on blood causes a blood strand to circulate inside the body [16]. The combination of efficient dosage targeting, and blood flow obstruction makes these treatment approaches challenging. However, from previous published articles, only few researchers did research on mixture of gold nanoparticle and magnetic nanoparticles. Thus, this research is done to investigate the relationship between gold nanoparticles together with magnetite nanoparticles. The mixture's multifunctional characteristics and prospective applications in analytical chemistry and nanomedicine have piqued the curiosity of nanomaterial experts.

Human blood, according to Rosli *et al.,* [17], is a non-Newtonian fluid that acts as pseudoplastic because it comprises ferrous ions that are magnetically sensitive and haemoglobin. Considering pseudoplastic boundary layer flow is incredibly beneficial to industry, research on this topic is very advantageous to both science and technology. The standard Navier-Stokes equations were unable to adequately characterise the pseudoplastic characteristics because of its pseudoplastic nature. As a result, it must be altered to depict the blood flow model. There are variety of fluid that is suitable to represent blood flow including Casson fluid. Casson's fluid flow analysis has been examined by several scientists, engineers, mathematicians, and researchers depending on various conditions. For example, Srivastava [18] investigated the Casson fluid model's pulsatile blood flow in an inclined artery under stenotic conditions caused by a magnetic field analytically. In order to study the blood flow in restricted small arteries, Nagarani and Sarojamma [19] modelled the blood as a Casson fluid. However, it is very few researchers who have covered on Williamson fluid. Williamson was the first to model the equation and circumstances of the pseudoplastic fluid [20]. Non-Newtonian fluids called Williamson nanofluids are utilised in several engineering procedures. The Williamson fluid, which has a better thermal property than its conventional ferrofluid competitors, is represented by blood. Heat transfer might be enhanced by adding nanoparticles to the base fluid. Loganathan and Sangeetha's [20] studies, which looked at how nanoparticles floating in Williamson fluid boost heat conductivity and mass transfer rate over a semi-infinite vertical plate, are among the most recent studies on Williamson fluid heat transfer. Maaitah *et al.,* [21] examined the impact of forced viscous dissipation on the characteristics of heat transmission and Williamson fluid flow when a horizontal plate is

passed through a saturated porous material at a constant surface temperature. Additionally, a lot of scholars have been interested in Williamson fluid's boundary layer properties on semi-infinite solid surfaces due to its various applications in the domains of fluid mechanics, heat transfer, and aerodynamics [22-26].

Few studies have been conducted to date on the thermal conductivity of magnetic core-shell nanoparticles for heat transfer applications, even though nanofluids based on non-magnetic nanoparticles are extensively researched. This statement is also supported by Imran *et al.,* [27] who studied on Carbon coated magnetite ferroparticles. Thus, this research intends to fill the knowledge gap by investigating magnetohydrodynamic free convective flow of Williamson hybrid ferrofluid on a horizontal circular cylinder in the presence of viscous dissipation. Since this research offers mathematical theory and a numerical technique for computations, it may find application in the industrial sector. Gold *(Au)* and magnetite ferroparticles (*Fe_3O_4*) are the nanoparticles that were taken into consideration for this study subsequently previous research muchly focus on other hybrid nanofluid without considering magnetite ferroparticles. In theory, adding a small amount of magnetite and gold nanoparticles to a non-Newtonian fluid should improve its thermal properties, keep it friction-free and fluid, and provide additional benefits from the gold and magnetite nanoparticles, such as acting as a hygienic controller agent. Currently, there is a lack of experimental evidence and theoretical analysis to support such an explanation. Future developments of hybrid ferrofluid will benefit from the understanding and validation of the fluid characteristics offered by the study findings. Therefore, the objective of this study is to solve the equations numerically using the Keller-box technique, an implicit finite difference methodology. Many properties are analysed and their implications on fluid flow are discussed, including the skin friction coefficient and Nusselt number.

2. Methodology

In this research, the geometry for the fluid is focusing on a horizontal circular cylinder with a radius of *a.* It is heated to a constant temperature, T_w, concurrently. As seen in Figure 1, the cylinder is immersed in a hybrid ferrofluid that is at room temperature, T_∞. The orthogonal coordinates, $\bar{x}$ and $\bar{y}$ are points along the cylinder surface that start at the lowest stagnation point, $\bar{x}=0,$ and go normal to it, respectively. Furthermore, it is assumed that the cylinder surface receives a uniformly normal magnetic field, B_o. The induced magnetic field is negligible since a low magnetic Reynolds number is predicted. Under the assumption that the boundary layer approximation is valid, the dimensional governing equations of steady free convection boundary layer flow are [28,29].

$$\frac{\partial \bar{u}}{\partial \bar{x}}+\frac{\partial \bar{v}}{\partial \bar{y}}=0, \tag{1}$$

$$\bar{u}\frac{\partial \bar{u}}{\partial \bar{x}}+\bar{v}\frac{\partial \bar{u}}{\partial \bar{y}}=\nu_{hnf}\frac{\partial^2 \bar{u}}{\partial \bar{y}^2}+\sqrt{2}\ \nu_{hnf}\Gamma\frac{\partial \bar{u}}{\partial \bar{y}}\frac{\partial^2 \bar{u}}{\partial \bar{y}^2}+\frac{(\rho\beta)_{hnf}}{\rho_{hnf}}g(T-T_\infty)\sin\frac{\bar{x}}{a}-\frac{\sigma_{hnf}B_o^2}{\rho_{hnf}}\bar{u}, \tag{2}$$

$$\bar{u}\frac{\partial T}{\partial \bar{x}}+\bar{v}\frac{\partial T}{\partial \bar{y}}==\frac{k_{hnf}}{(\rho C_p)_{hnf}}\frac{\partial^2 T}{\partial \bar{y}^2}+\frac{\mu_{hnf}}{(\rho C_p)_{hnf}}\left(\frac{\partial \bar{u}}{\partial \bar{y}}\right)^2, \tag{3}$$

Subjected to the following boundary conditions

$$\bar{u}(\bar{x},0)=\bar{v}(\bar{x},0)=0,\quad T(\bar{x},0)=T_w,\quad \bar{u}(\bar{x},\infty)\to 0,\quad T(\bar{x},\infty)\to T_\infty, \tag{4}$$

From the above equations, $\bar{u}$ and $\bar{v}$ represented the velocity along the $\bar{x}$ and $\bar{y}$ axes, respectively. Meanwhile, the presence of hybrid ferrofluid's kinematic viscosity, hybrid nanofluid density, hybrid ferrofluid thermal expansion as well as hybrid dynamic viscosity are illustrated by ν_{hnf}, ρ_{hnf}, β_{hnf} and μ_{hnf} respectively. g denotes the gravitational acceleration forced on the fluid flow. T is the local temperature. Next, $\left(\rho C_p\right)_{hnf}$ is the heat capacity of hybrid ferrofluid and k_{hnf} depicts the hybrid ferrofluid's thermal conductivity. In addition, the homogeneous magnetic field intensity and electrical conductivity are indicated by β_o and σ_{hnf}, consequently.

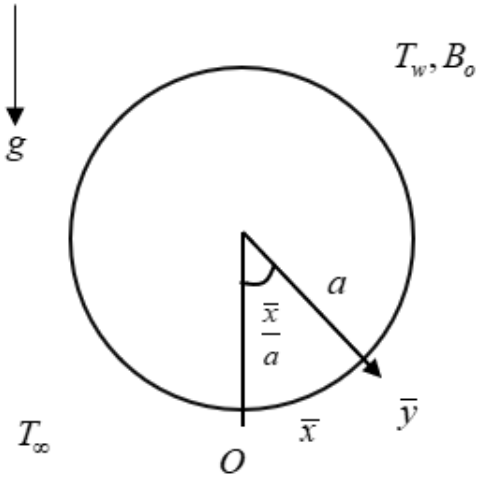

Fig. 1. Physical model and the coordinate system

Since there are multiple particles involved in the fluid flow, each subscript is an indication of each particle. Specifically, $_{bf}$,$_{hnf}$ and $_{s1,s2}$ are the qualities if the base fluid, hybrid ferrofluid, and gold along with ferromagnetic nanoparticles, respectively. Moreover, the solid volume fraction, ϕ is as follows [24,25].

$$\nu_{hnf}=\frac{\mu_{hnf}}{\rho_{hnf}},\ \mu_{hnf}=\frac{\mu_f}{(1-\phi_1)^{2.5}(1-\phi_2)^{2.5}},\ \rho_{hnf}=(1-\phi_2)\left[(1-\phi_1)\rho_f+\phi_1\rho_{s1}\right]+\phi_2\rho_{s2},$$

$$\left(\rho\beta\right)_{hnf}=(1-\phi_2)\left[(1-\phi_1)\left(\rho\beta\right)_f+\phi_1\left(\rho\beta\right)_{s1}\right]+\phi_2\left(\rho\beta\right)_{s2},$$

$$\left(\rho C_p\right)_{hnf}=(1-\phi_2)\left[(1-\phi_1)\left(\rho C_p\right)_f+\phi_1\left(\rho C_p\right)_{s1}\right]+\phi_2\left(\rho C_p\right)_{s2},$$

$$\frac{k_{hnf}}{k_{bf}}=\frac{k_{s2}+2k_{bf}-2\phi_2(k_{bf}-k_{s2})}{k_{s2}+2k_{bf}+\phi_2(k_{bf}-k_{s2})},\quad \frac{k_{bf}}{k_f}=\frac{k_{s1}+2k_f-2\phi_1(k_f-k_{s1})}{k_{s1}+2k_f+\phi_1(k_f-k_{s1})},$$

$$\frac{\sigma_{hnf}}{\sigma_{bf}}=\frac{\sigma_{s2}+2\sigma_{bf}-2\phi_2(\sigma_{bf}-\sigma_{s2})}{\sigma_{s2}+2\sigma_{bf}+\phi_2(\sigma_{bf}-\sigma_{s2})},\quad \frac{\sigma_{bf}}{\sigma_f}=\frac{\sigma_{s1}+2\sigma_f-2\phi_1(\sigma_f-\sigma_{s1})}{\sigma_{s1}+2\sigma_f+\phi_1(\sigma_f-\sigma_{s1})}.$$

Due to having a dimensional governing equation, thus the suitable non-dimensional variables are introduced.

$$x=\frac{\overline{x}}{a},\quad y=Gr^{1/4}\frac{\overline{y}}{a},\quad u=\frac{a}{\nu_f}Gr^{-1/2}\overline{u},\quad v=\frac{a}{\nu_f}Gr^{-1/4}\overline{v},\quad \theta(\eta)=\frac{T-T_\infty}{T_w-T_\infty}. \tag{5}$$

where the θ and $Gr=\dfrac{g\beta_f(T_w-T_\infty)a^3}{\nu_f{}^2}$ presenting the dimensionless fluid's temperature and Grashof number, respectively. Eq. (5) is used to simplify the governing equations (1) through (4) and the boundary conditions to non-dimensional equations.

$$\frac{\partial u}{\partial x}+\frac{\partial v}{\partial y}=0, \tag{6}$$

$$u\frac{\partial u}{\partial x}+v\frac{\partial u}{\partial y}=\frac{\nu_{hnf}}{\nu_f}\frac{\partial^2 u}{\partial y^2}+\frac{\sqrt{2}\Gamma\nu_f Gr^{3/4}}{a^2}\frac{\partial u}{\partial y}\frac{\partial^2 u}{\partial y^2}+\frac{(\rho\beta)_{hnf}}{\rho_{hnf}\beta_f}\theta\sin x-\frac{\sigma_{hnf}a^2}{\rho_{hnf}\nu_f Gr^{1/2}}B_o^2 u, \tag{7}$$

$$u\frac{\partial\theta}{\partial x}+v\frac{\partial\theta}{\partial y}=\frac{k_{hnf}}{\nu_f(\rho C_p)_{hnf}}\frac{\partial^2\theta}{\partial y^2}+\frac{\nu_{hnf}\rho_{hnf}\nu_f Gr}{\left(\rho C_p\right)_{hnf}\left(T_w-T_\infty\right)a^2}\left(\frac{\partial u}{\partial y}\right)^2, \tag{8}$$

where the equations are now subjected to

$$u(x,0)=v(x,0)=0,\quad \theta(x,0)=1,\quad u(x,\infty)\to 0,\quad \theta(x,\infty)\to 0, \tag{9}$$

In addition, the fact that the several dependent variables in Eq. (6) through Eq. (9) making the equations challenging to solve, the following similarity functions are introduced.

$$\psi=xf(x,y),\quad \theta=\theta(x,y), \tag{10}$$

The stream function is designated by ψ. It is described as $u=\dfrac{\partial\psi}{\partial y}$ and $v=-\dfrac{\partial\psi}{\partial x}$ that satisfied Eq. (6) accurately. The subsequent partial differential equations are formed by substituting Eq. (10) into Eq. (6) to Eq. (8)

$$\begin{aligned}&\frac{\nu_{hnf}}{\nu_f}\frac{\partial^3 f}{\partial y^3}+\frac{\nu_{hnf}}{\nu_f}We\frac{\partial^2 f}{\partial y^2}\frac{\partial^3 f}{\partial y^3}+f\frac{\partial^2 f}{\partial y^2}-\left(\frac{\partial f}{\partial y}\right)^2+\frac{(\rho\beta)_{hnf}}{\rho_{hnf}\beta_f}\frac{\sin x}{x}\theta-\frac{\rho_f\sigma_{hnf}}{\rho_{hnf}\sigma_f}M\frac{\partial f}{\partial y}\\&=x\left(\frac{\partial f}{\partial y}\frac{\partial^2 f}{\partial x\partial y}-\frac{\partial f}{\partial x}\frac{\partial^2 f}{\partial y^2}\right),\end{aligned} \tag{11}$$

$$\frac{k_{hnf}(\rho C_p)_f}{k_f(\rho C_p)_{hnf}}\frac{1}{\Pr}\frac{\partial^2\theta}{\partial y^2}+f\frac{\partial\theta}{\partial y}=x\left(\frac{\partial f}{\partial y}\frac{\partial\theta}{\partial x}-\frac{\partial f}{\partial x}\frac{\partial\theta}{\partial y}-xEc\frac{\nu_{hnf}}{\nu_f}\frac{\rho_{hnf}\left(C_p\right)_f}{\left(\rho C_p\right)_{hnf}}\left(\frac{\partial^2 f}{\partial y^2}\right)^2\right). \tag{12}$$

The boundary conditions are transformed and applied to the equations.

$$f(x,0)=\frac{\partial f}{\partial y}(x,0)=0,\quad \theta(x,0)=1,\quad \frac{\partial f}{\partial y}(x,\infty)\to 0,\quad \theta(x,\infty)\to 0, \tag{13}$$

By definition, $M=\frac{\sigma_f a^2 B_o^2}{\rho_f \nu_f Gr^{1/2}}$ is the magnetic parameter, $We=\frac{\sqrt{2}x\Gamma \nu_f Gr^{3/4}}{a^2}$ is the Williamson parameter, $Ec=\frac{{\nu_f}^2 Gr}{a^2\left(C_p\right)_f\left(T_w-T_\infty\right)}$ is an Eckert number, and $\Pr=\frac{\nu_f\left(\rho C_p\right)_f}{k_f}$ is the Prandtl number. The details of other hybrid ferrofluid quantities are provided below

$$\frac{\nu_{hnf}}{\nu_f}=\frac{1}{(1-\phi_1)^{2.5}(1-\phi_2)^{2.5}\left[(1-\phi_2)+\left[(1-\phi_1)+\phi_1(\rho_{s1}/\rho_f)\right]+\phi_2(\rho_{s2}/\rho_f)\right]},$$

$$\frac{(\rho\beta)_{hnf}}{\rho_{hnf}\beta_f}=\frac{(1-\phi_2)\left[(1-\phi_1)\rho_f+\phi_1(\rho\beta)_{s1}/\beta_f\right]+\phi_2(\rho\beta)_{s2}/\beta_f}{(1-\phi_2)\left[(1-\phi_1)\rho_f+\phi_1\rho_{s1}\right]+\phi_2\rho_{s2}},$$

$$\frac{k_{hnf}(\rho C_p)_f}{k_f(\rho C_p)_{hnf}}=\frac{k_{hnf}/k_f}{(1-\phi_2)\left[(1-\phi_1)+\phi_1(\rho C_p)_{s1}/(\rho C_p)_f\right]+\phi_2(\rho C_p)_{s2}/(\rho C_p)_f},$$

$$\frac{\rho_{hnf}\left(C_p\right)_f}{\left(\rho C_p\right)_{hnf}}=\frac{(1-\phi_2)\left[(1-\phi_1)\rho_f+\phi_1\rho_{s1}\right]+\phi_2\rho_{s2}}{(1-\phi_2)\left[(1-\phi_1)\rho_f+\phi_1\left(\rho C_p\right)_{s1}/\left(C_p\right)_f\right]+\phi_2\left(\rho C_p\right)_{s2}/\left(C_p\right)_f},$$

$$\frac{\rho_f\sigma_{hnf}}{\rho_{hnf}\sigma_f}=\frac{\sigma_{hnf}/\sigma_f}{(1-\phi_2)\left[(1-\phi_1)+\phi_1\rho_{s1}/\rho_f\right]+\phi_2\rho_{s2}/\rho_f}.$$

The physical variables that are interested to be analysed in this research are the skin friction coefficient, C_f and the local Nusselt number, Nu_x which are provided by

$$C_f=\frac{\tau_w}{\rho_f u_\infty^2},\quad Nu_x=\frac{aq_w}{k_f(T_w-T_\infty)}, \tag{14}$$

From Eq. (14), the surface shear stress, τ_w and the surface heat flow, q_w are determined to be as follows

$$\tau_w=\mu_{hnf}\left(\frac{\partial\bar{u}}{\partial\bar{y}}+\frac{\Gamma}{\sqrt{2}}\left(\frac{\partial\bar{u}}{\partial\bar{y}}\right)^2\right)_{\bar{y}=0},\quad q_w=-k_{hnf}\left(\frac{\partial T}{\partial\bar{y}}\right)_{\bar{y}=0}, \tag{15}$$

Eq. (15) simplifies the equations in (14) by utilising variables.

$$C_f Gr^{1/4} = \frac{1}{(1-\phi_1)^{2.5}(1-\phi_2)^{2.5}}\left(x\frac{\partial^2 f}{\partial y^2} + \frac{We}{2}x\left(\frac{\partial^2 f}{\partial y^2}\right)^2 \right)_{\bar{y}=0}, \quad Nu_x Gr^{-1/4} = -\frac{k_{hnf}}{k_f}\left(\frac{\partial \theta}{\partial y}\right)_{\bar{y}=0}, \tag{16}$$

Furthermore, the temperature profile and velocity profile may be determined through the following relations, correspondingly.

$$u = f'(x,y), \quad \theta = \theta(x,y), \tag{17}$$

In simplest understanding, the method of this problem can be display in a flowchart as shown in Figure 2 below.

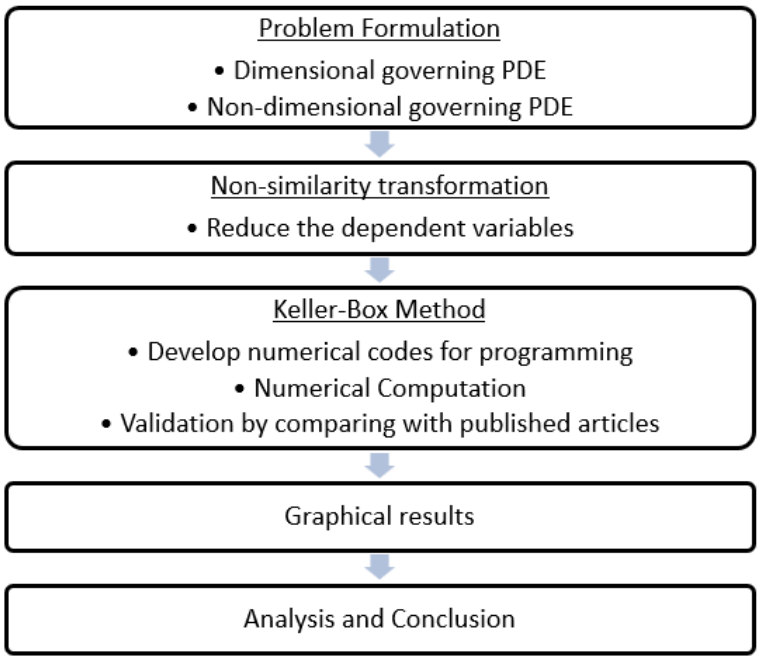

Fig. 2. Research operational framework

3. Results and Discussion

The resultant equations are numerically solved using the Keller-box method approach, also known as the implicit finite difference technique. Newton's technique is suitable for solving parabolic differential equations that are nonlinear at any order and is unconditionally stable due to its linearization. The Keller-box method's approach is coded using MATLAB software for numerical computing, resulting in the velocity and temperature profile findings. Since blood is the fundamental fluid in this investigation, $\Pr$ is set at 21. In accordance with Devi and Devi [30], blood is first mixed with 0.1 volume solid Fe_3O_4, $(\phi_1 = 0.1)$ nanoparticles to create a Fe_3O_4-blood ferrofluid. Subsequently, *Fe_3O_4*-blood ferrofluid is mixed with 0.06 volume solid gold, Au, $(\phi_2 = 0.06)$ nanoparticles to create *Fe_3O_4-Au*/Blood hybrid ferrofluid. It should be mentioned that the boundary layer thickness is set to 10 with a step size of $\Delta x = 0.01$ and $\Delta y = 0.02$ is used in order to obtain a convergent and accurate numerical result. This section presents graphical results of various values of nanoparticles, Williamson parameter and magnetic parameter towards physical quantities interested.

The thermophysical properties of blood, gold (Au), and magnetite particles (Fe_3O_4) are displayed in Table 1. The numerical outcomes and the results from the previous investigation were reviewed. The current study is simplified to earlier research for comparison's sake. Consequently, it shows that the results of the present investigation are highly compatible with a study carried out by [8,31,32]. Table 2 and Table 3 tabulate the results of the comparison.

Table 1
Thermophysical characteristics of blood, magnetic ferroparticles and gold

Physical Properties	Blood	Ferrite, Fe_3O_4 (ϕ_1)	Gold, Au (ϕ_2)
Solid Volume Fraction $\rho\ (\mathrm{kg/m^3})$	1063	5180	19300
Specific Heat Capacity of Solid $C_p\ (\mathrm{J/kg.K})$	3594	670	129.1
Solid Thermal Conductivity $k\ (\mathrm{W/m.K})$	0.492	9.7	318
Solid Thermal Expansion Coefficient $(1/\mathrm{K})$	0.000021	0.0000148	0.000013
Electrical Conductivity $\sigma\ (1/\Omega m)$	0.8	25000	4100000

Table 2
Comparison of $Nu_x Gr^{-1/4}$ with published articles

x	$Nu_x Gr^{-1/4}$			
	Merkin [31]	Molla *et al.,* [32]	Mohamed *et al.,* [8]	Present
0	0.4214	0.4214	0.4213	0.4213
$\frac{\pi}{6}$	0.4161	0.4163	0.4161	0.4161
$\frac{\pi}{3}$	0.4007	0.4005	0.4007	0.4008
$\frac{\pi}{2}$	0.3745	0.3740	0.3743	0.3740
$\frac{2\pi}{3}$	0.3364	0.3355	0.3359	0.3360
$\frac{5\pi}{6}$	0.2825	0.2812	0.2815	0.2815
π	0.1945	0.1917	0.1934	0.1921

Table 3
Comparison of $C_f Gr^{1/4}$ with published articles

x	$C_f Gr^{1/4}$			
	Merkin [31]	Molla *et al.,* [32]	Mohamed *et al.,* [8]	Present
0	0.0000	0.0000	0.0000	0.0000
$\frac{\pi}{6}$	0.4151	0.4145	0.4156	0.4150
$\frac{\pi}{3}$	0.7558	0.7539	0.7534	0.7532
$\frac{\pi}{2}$	0.9579	0.9541	0.9557	0.9557
$\frac{2\pi}{3}$	0.9756	0.9696	0.9726	0.9732
$\frac{5\pi}{6}$	0.7822	0.7739	0.7773	0.7758
π	0.3391	0.3264	0.3356	0.3251

This research examines and focusing on the impact of ϕ_1 and ϕ_2, M and We in relation to skin friction parameter, $C_f Gr^{1/4}$, the local Nusselt number, $Nu_x Gr^{-1/4}$, the temperature profile, $\theta(y)$, together with the velocity profile, $f'(y)$.

The effects of varied ϕ_1 and ϕ_2 values are shown in Figure 3 to Figure 6. It was found from Figure 3 that there was no friction $\left(C_f Gr^{1/4} = 0\right)$ at the stagnation area $\left(x = 0\ rad\right)$. As the fluid passes through the centre of the circular cylinder, the $C_f Gr^{1/4}$ rises and eventually descends to the surface of the cylinder. Figure 3 illustrates how incorporating Fe_3O_4 ferroparticles to a blood-based fluid results in an increase in the value of $C_f Gr^{1/4}$ which forming a Fe_3O_4-blood ferrofluid $\left(\phi_1 = 0.1,\ \phi_2 = 0.0\right)$. Then, in comparison to all other ferrofluids tested, including the Fe_3O_4-blood ferrofluid $\left(\phi_1 = 0.16,\ \phi_2 = 0.0\right)$, the greatest $C_f Gr^{1/4}$ values were obtained when 0.06 vol of *Au* nanoparticles were blended with the ferrofluid to generate the Fe_3O_4-Au/Blood hybrid ferrofluid $\left(\phi_1 = 0.1,\ \phi_2 = 0.06\right)$. In terms of physical density, Fe_3O_4 ferroparticles in Fe_3O_4-blood ferrofluid $\left(\phi_1 = 0.16,\ \phi_2 = 0.0\right)$, are less dense than *Au* nanoparticles in Fe_3O_4-Au/Blood hybrid ferrofluid $\left(\phi_1 = 0.1,\ \phi_2 = 0.06\right)$. Consequently, the great relevance in fluid-cylinder surface friction was provided.

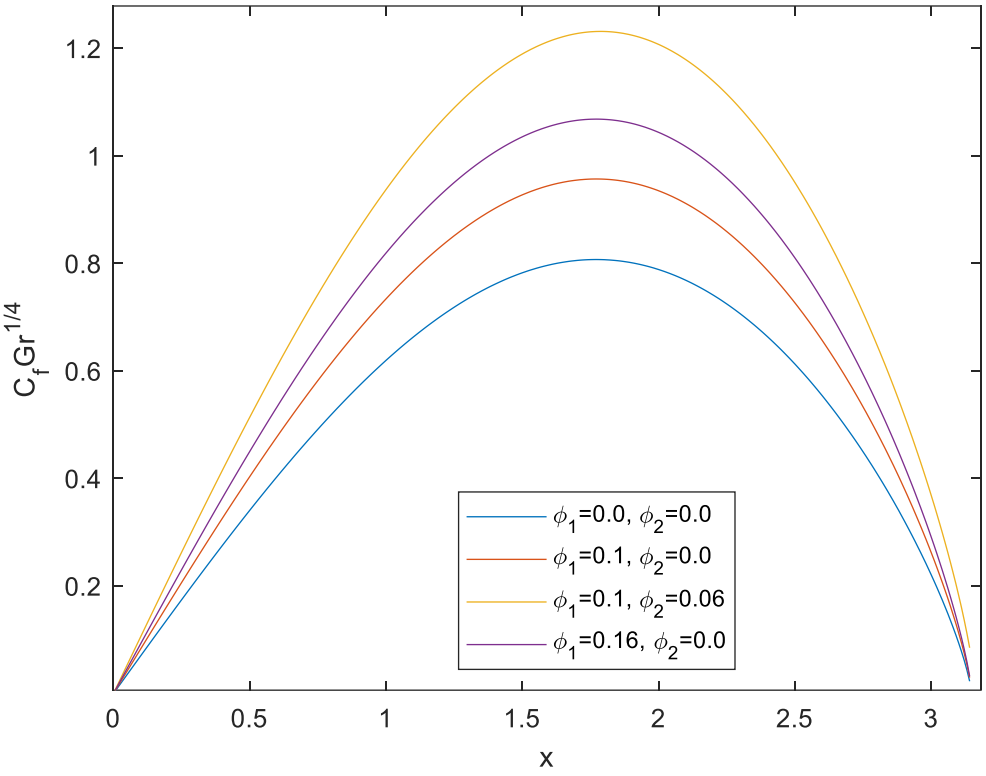

Fig. 3. Skin Friction coefficient, $C_f Gr^{1/4}$ variation versus *x* for different ϕ_1 and ϕ_2

The variation of the $Nu_x Gr^{-1/4}$ for various values of ϕ_1 and ϕ_2 is analysed in Figure 4. It was demonstrated that the stagnation zone had the greatest influence on the volume fractions of different ferroparticles. The fluid's thermal conductivity was enhanced by the addition of nanoparticles, which increased the $Nu_x Gr^{-1/4}$ values. The blood-based fluid $(\phi_1 = 0.0,\ \phi_2 = 0.0)$ had the lowest $Nu_x Gr^{-1/4}$ score, according to Figure 4. The levels of $Nu_x Gr^{-1/4}$ have increased due to the presence of Fe_3O_4 in blood, which is represented as Fe_3O_4-blood ferrofluid $(\phi_1 = 0.1,\ \phi_2 = 0.0)$. The convective heat transfer capacities of the Fe_3O_4-Au/Blood hybrid ferrofluid $(\phi_1 = 0.1,\ \phi_2 = 0.06)$ have been improved by blending it with gold nanoparticles. $Nu_x Gr^{-1/4}$ has increased due in part to *Au*'s excellent thermal conductivity, which has physically translated to an increase in thermal convective abilities. It may be observed that the $Nu_x Gr^{-1/4}$ values acquired are superior than the ferrofluid made by Fe_3O_4-blood ferrofluid $(\phi_1 = 0.16,\ \phi_2 = 0.0)$. Moreover, the values of $Nu_x Gr^{-1/4}$ reduce towards the end of the cylinder surface as the fluid flow crosses the cylindrical surface, indicating a decrease in convective heat transfer capacities and an increase in conductive effects.

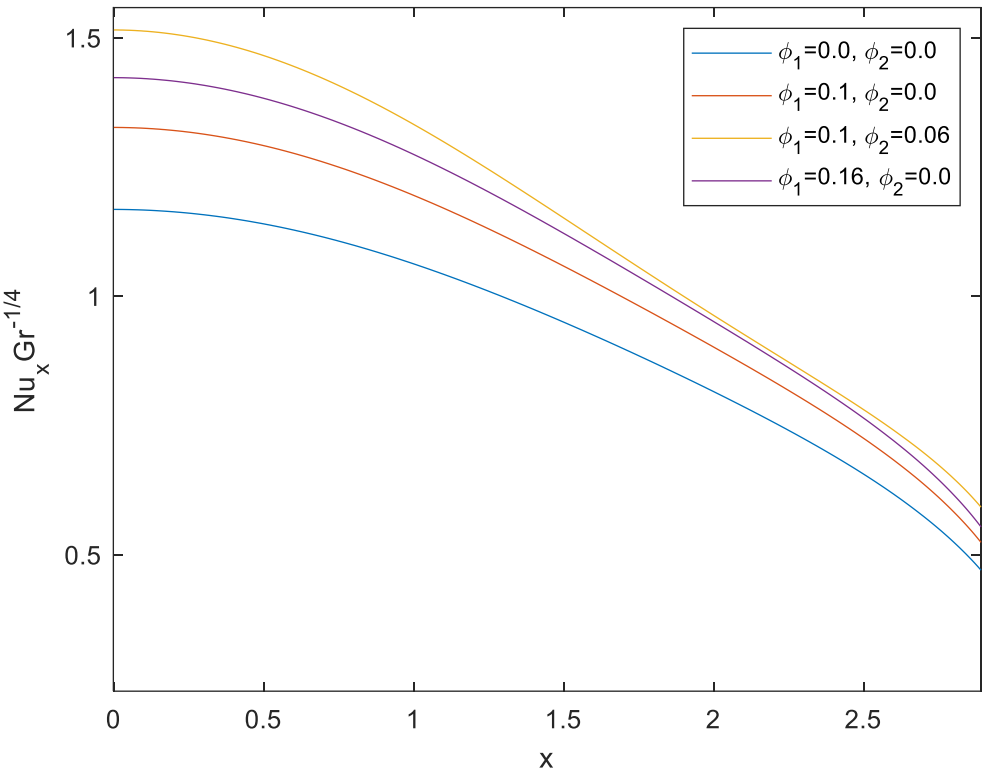

Fig. 4. Nusselt number, $Nu_x Gr^{-1/4}$ variation versus *x* for different ϕ_1 and ϕ_2

The temperature profile, $\theta(y)$, and velocity profile, $f'(y)$, are displayed in Figure 5 and Figure 6, respectively. The thickness of the boundary layer is very minimally changed by both profiles. The fluid's increased nanoparticle content in Figure 5 caused the thermal boundary layer thickness to slightly rise. The fluid flow's thermal conductivity has risen due to the presence of nanoparticles; this has raised the fluid's thermal diffusivity, which has increased the thickness of the thermal boundary layer.

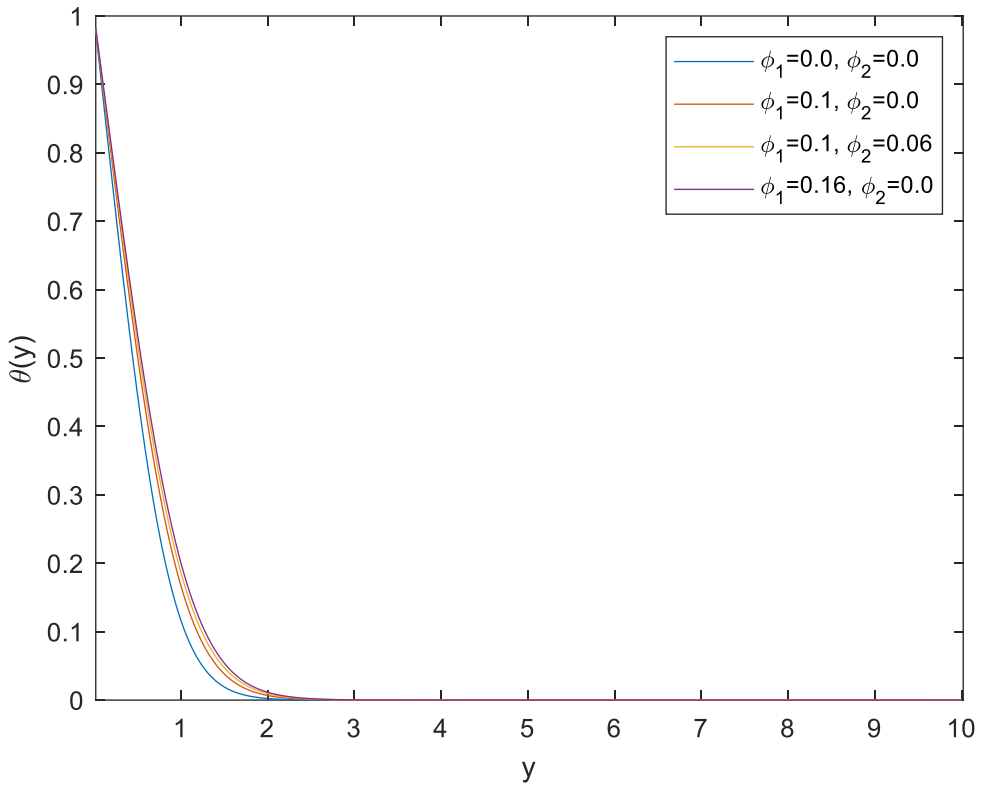

Fig. 5. Temperature profile, $\theta(y)$ variation versus *y* for different ϕ_1 and ϕ_2

In Figure 6, on the other hand, the presence of nanoparticles in the fluid flow has led to an improvement in momentum, which in turn has enhanced velocity indirectly. Furthermore, the Fe_3O_4-Au/Blood hybrid ferrofluid $(\phi_1 = 0.1,\ \phi_2 = 0.06)$ with higher fluid density decelerates faster than the Fe_3O_4-blood ferrofluid $(\phi_1 = 0.16,\ \phi_2 = 0.0)$ when comparing the fluid with the same percentage of nanoparticles. This is caused by the boundary layer's diminishing thickness, which, as Figure 3 illustrates, physically represents the fluid's and the cylinder's rising friction.

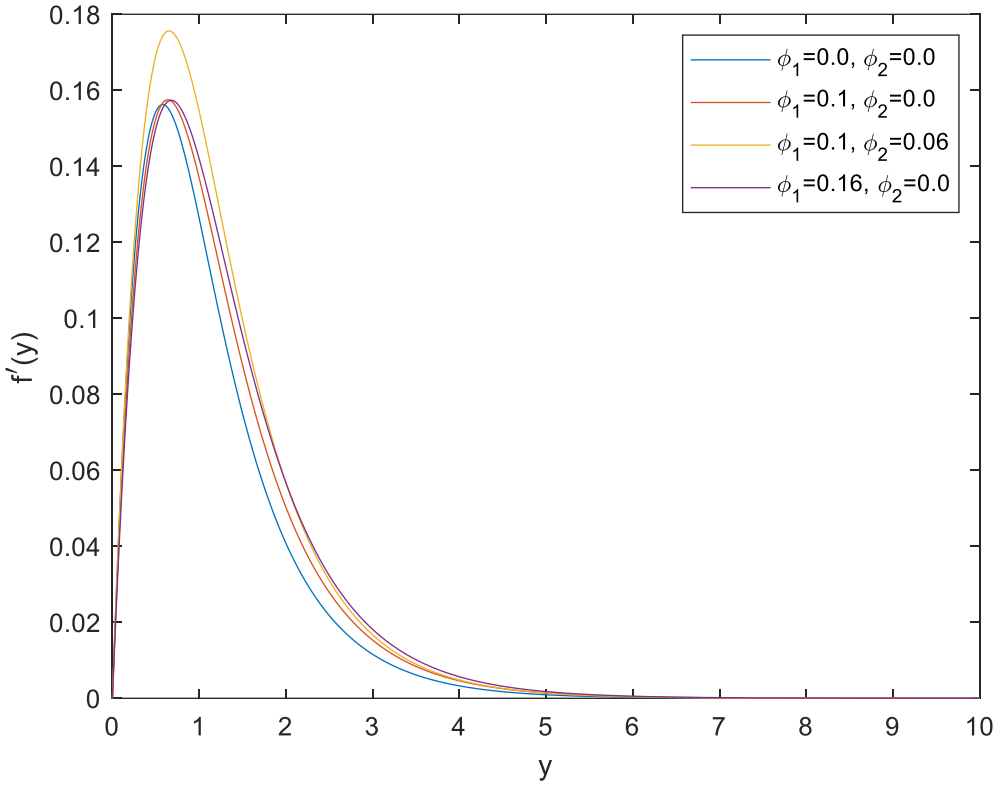

Fig. 6. Velocity profile, $f'(y)$ variation versus *y* for different ϕ_1 and ϕ_2

Figure 7 to Figure 10 depict the implications of *M* on the flow of the Fe_3O_4-Au/Blood hybrid ferrofluid $(\phi_1 = 0.1,\ \phi_2 = 0.06)$. As the values of *M* develop, Figure 7 and Figure 8 show that $C_f Gr^{1/4}$ and $Nu_x Gr^{-1/4}$ both declines. As seen in Figure 10, an increase in *M* results in a drag force that slows down the fluid flow and lowers its velocity. Low velocity differences and gradients, which physically translated to low skin friction coefficient $\left(C_f Gr^{1/4}\right)$ have been attributed to this condition.

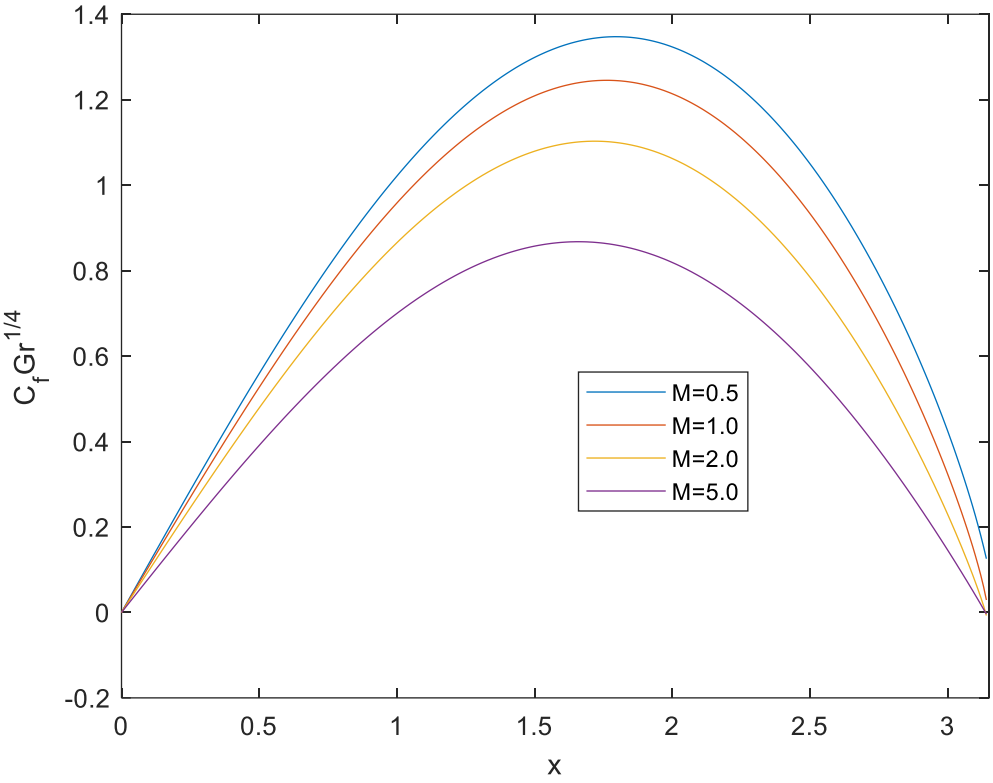

Fig. 7. Skin Friction coefficient, $C_f Gr^{1/4}$ variation versus *x* for different M

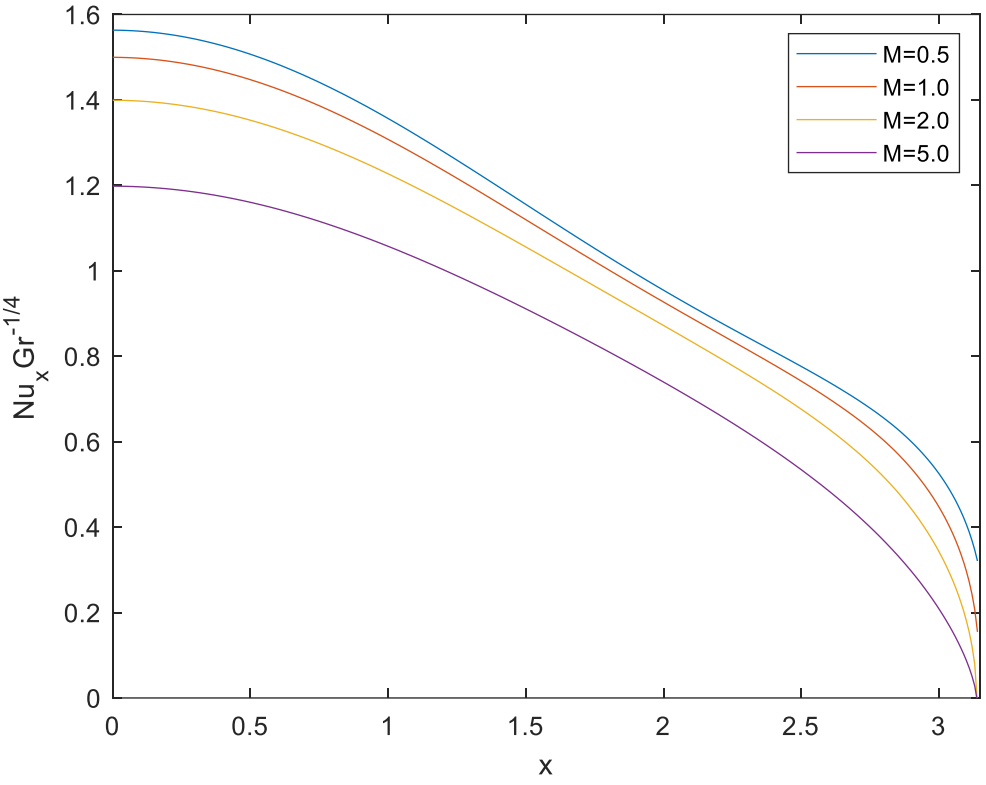

Fig. 8. Nusselt number, $Nu_x Gr^{-1/4}$ variation versus *x* for different M

Subsequently, Figure 9 and Figure 10 demonstrate how increasing *M* values cause the thermal boundary layer thickness to rise while decreasing the velocity boundary layer thickness. The fluid's ferroparticles are drawn to the cylinder surface by the Lorentz force, which in turn restricts the fluid's flow. Because of this circumstance, the fluid momentum has decreased, which has led to a weakening of the velocity boundary layer thickness. At the same time, this force produces a particular kind of friction that alters the flow and eventually boosts the temperature profile as seen in Figure 9 due to the additional heat energy that this friction produces.

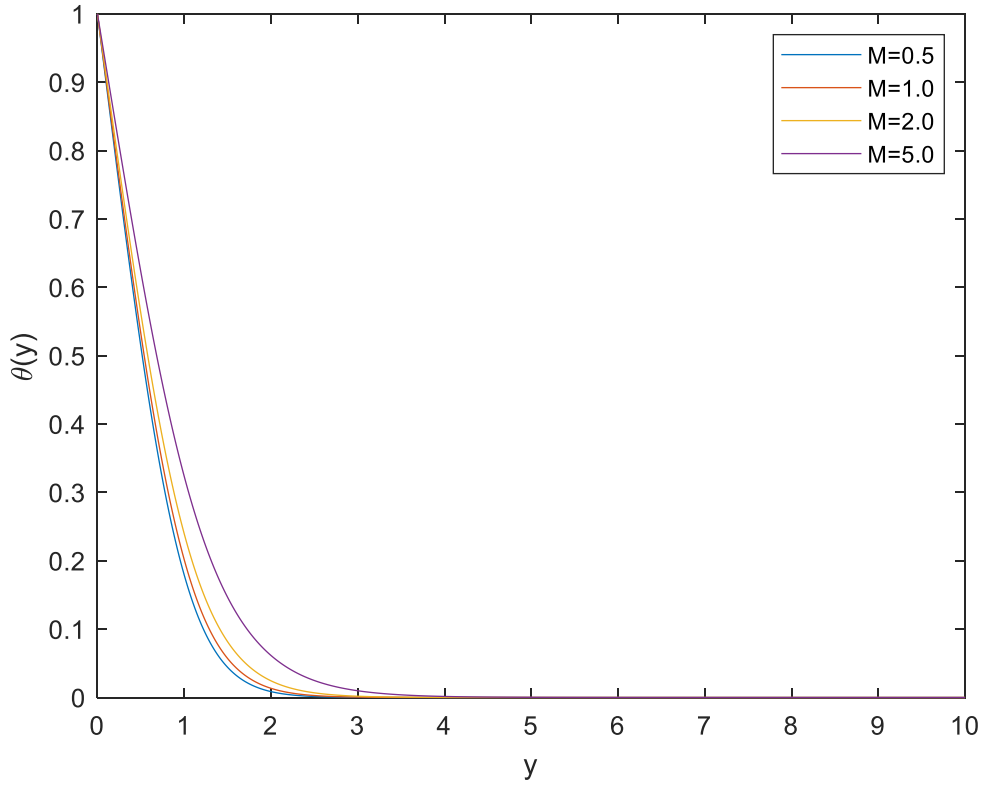

Fig. 9. Temperature profile, $\theta(y)$ variation versus *y* for different M

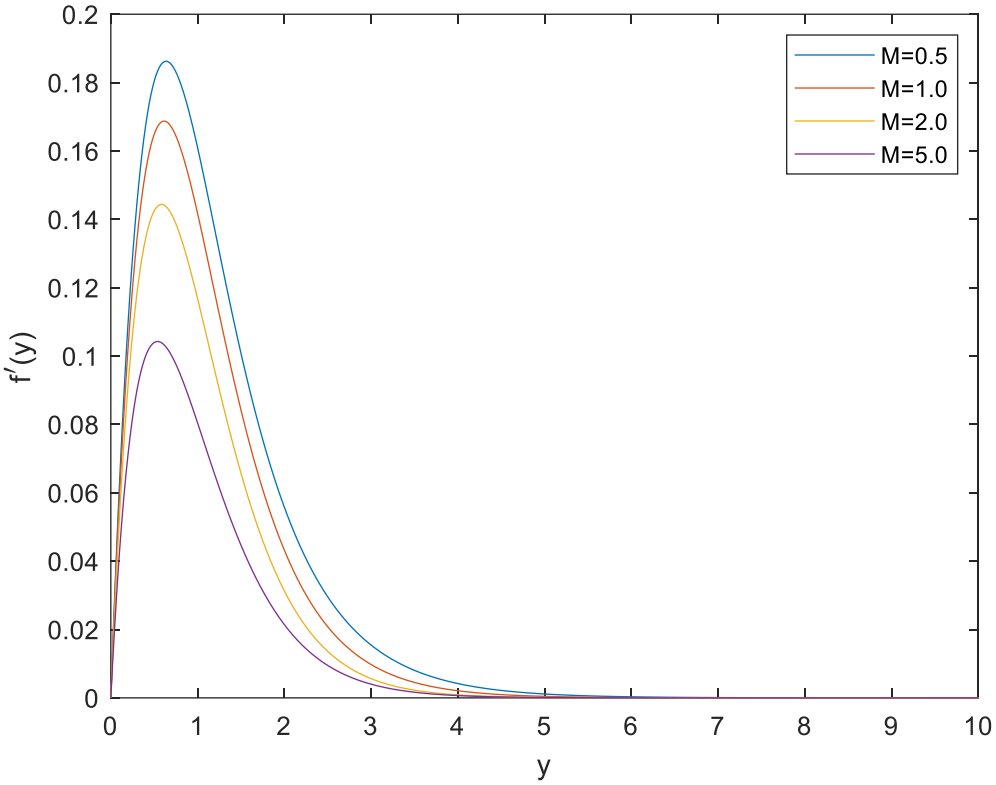

Fig. 10. Velocity profile, $f'(y)$ variation versus *y* for different M

Lastly, Figure 11 to Figure 14 illustrate the consequences of various values *We*. This value represents the relaxation to retardation time ratio. Theoretically, a rise in *We* would shorten the retardation period, which would raise the boundary layer's thickness and lower $f'(y)$. Figure 11 illustrates how a fluid's resistance to flow rises with *We*, leading to an increase in $C_f Gr^{1/4}$. In the meanwhile, Figure 12 illustrates the slight influence that *We* has on the $Nu_x Gr^{-1/4}$ outcomes. In considering the impact of *We* on $\theta(y)$ and $f'(y)$, Figure 13 and 14 depict the corresponding impacts. Both profiles exhibit a diminishing trend as the parameter of *We* increases. The fluid's temperature naturally rises when the We parameter increases because the relaxation period is longer.

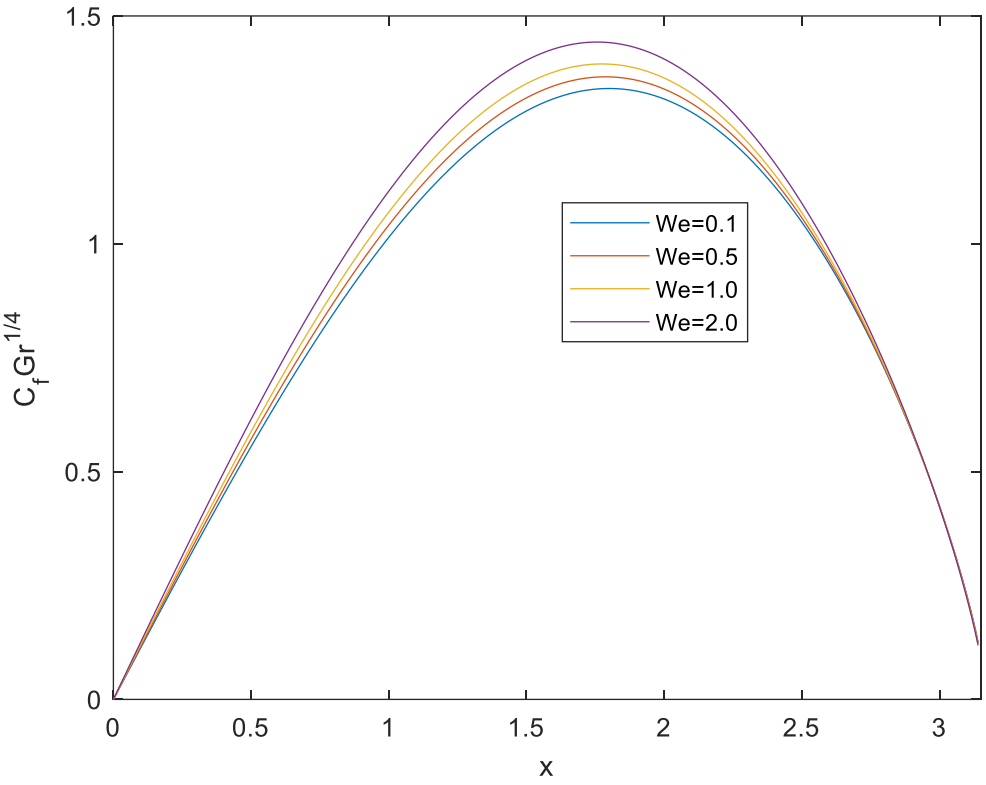

Fig. 11. Skin Friction coefficient, $C_f Gr^{1/4}$ variation versus *x* for different We

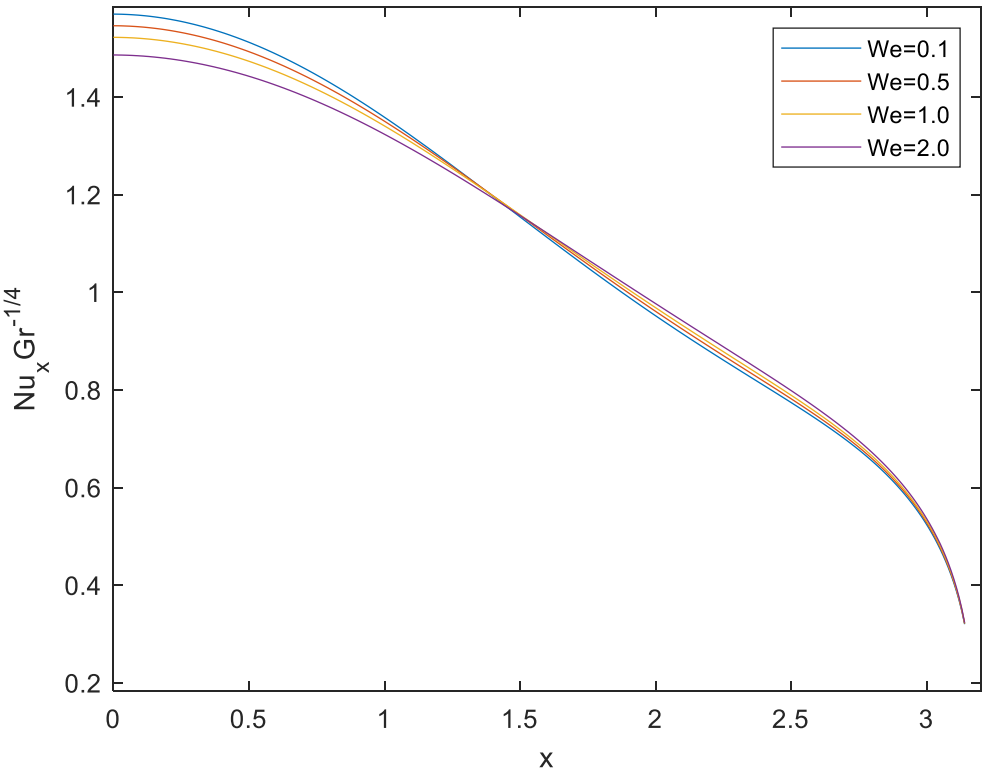

Fig. 12. Nusselt number, $Nu_x Gr^{-1/4}$ variation versus *x* for different We

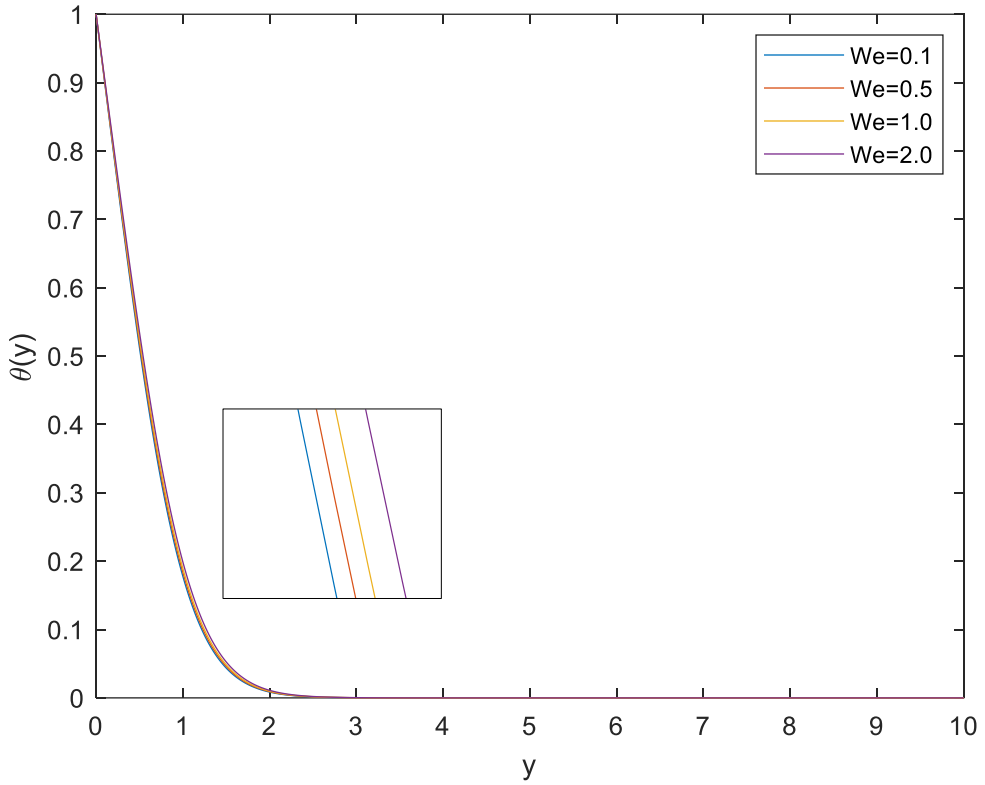

Fig. 13. Temperature profile, $\theta(y)$ variation versus *y* for different We

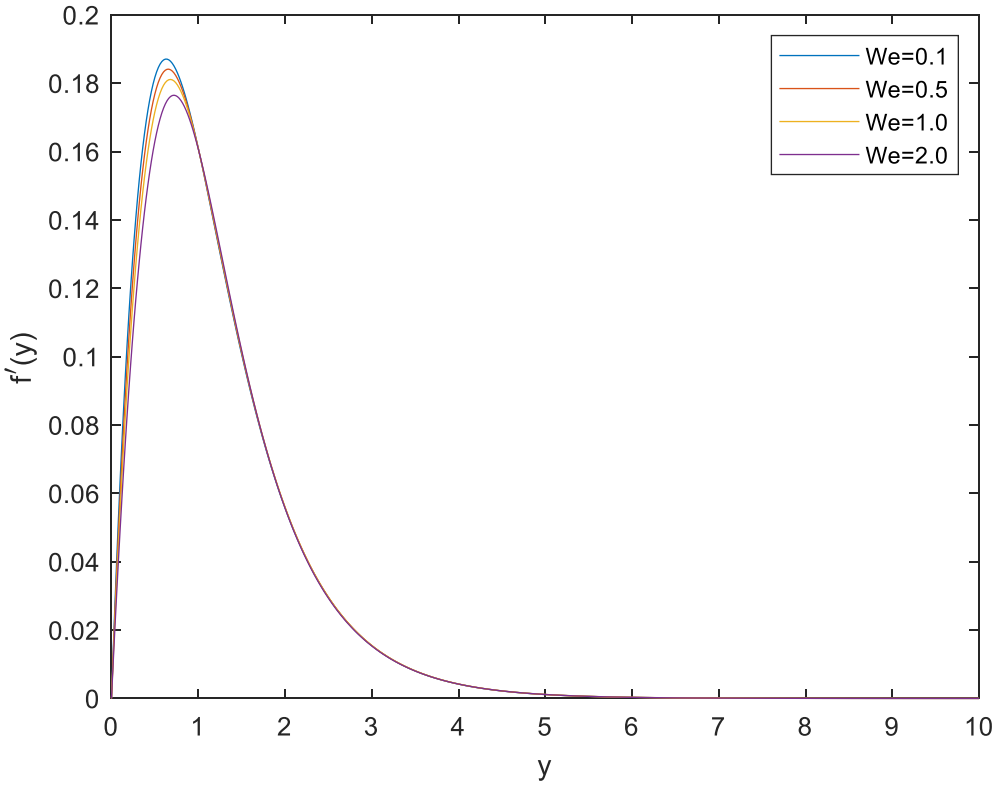

Fig. 14. Velocity profile, $f'(y)$ variation versus *y* for different We

4. Conclusions

The research offers a numerical analysis of the free convection boundary layer flow over a horizontal circular cylinder in a hybrid Williamson ferrofluid using the Keller-box method. It is demonstrated how the skin friction coefficient, Nusselt number, temperature profile, and velocity profile of the hybrid Williamson ferrofluid are affected by the volume percentage of ferrite and gold nanoparticles, the magnetic parameter, and the Williamson parameter. The main conclusion that can be make from this research is it is proven that the presence of magnetic ferroparticles in the fluid have improve the heat transfer as compared to a basic nanofluid. In addition, the hybrid ferrofluid performed better in terms of skin friction and convective heat transfer than ferrofluid with the same particle volume percent. A synopsis of the research that can be obtained from it is as follows

i. The increase in nanoparticles in the ferrofluid has resulted in an increase in both the skin friction coefficient and the Nusselt numbers.
ii. As the magnetic parameter increases, the Nusselt numbers and the skin friction coefficient drop.
iii. The thermal boundary layer thicknesses have increased while the velocity boundary layer has thinned due to the rise in magnetic parameter.
iv. This increase in the magnetic parameter's intensity reduces the drag forces brought on by the fluid velocity constraint brought about by Lorentz force production, which in turn lowers the fluid velocity and the skin friction coefficient.
v. The Williamson hybrid ferrofluid proven may have performed better in terms of convective heat transfer capacities with high friction between fluid and the cylinder surface when compared to ferrofluids with the same amount of nanoparticle volume fraction.

Additionally, this study may be expanded to different physical geometries, such a spherical coordinate system. Geometries of porous media must also be taken into account. A solid body with open space surrounding it to permit fluid to pass over or through it is called a porous medium. Porous media also has several advantages in the fields of agriculture, geothermal research, and building. As such, several studies might be conducted to link the fluid flow issue.

Acknowledgement

The author would like to acknowledge the financial support received from the Ministry of Higher Education Malaysia (FRGS/1/2023/STG06/UMP/02/1) (University reference: RDU230111) and Universiti Malaysia Pahang (PGRS2303143).

References

[1] Singh Mehta, Jaswinder, Rajesh Kumar, Harmesh Kumar, and Harry Garg. "Convective heat transfer enhancement using ferrofluid: a review." *Journal of Thermal Science and Engineering Applications* 10, no. 2 (2018): 020801. https://doi.org/10.1115/1.4037200

[2] Stephen, Papell Solomon. "Low viscosity magnetic fluid obtained by the colloidal suspension of magnetic particles." *U.S. Patent 3,215,572*, issued November 2, 1965.

[3] Oehlsen, Oscar, Sussy I. Cervantes-Ramírez, Pabel Cervantes-Avilés, and Illya A. Medina-Velo. "Approaches on ferrofluid synthesis and applications: current status and future perspectives." *ACS Omega* 7, no. 4 (2022): 3134-3150. https://doi.org/10.1021/acsomega.1c05631

[4] Jamaludin, Anuar, Kohilavani Naganthran, Roslinda Nazar, and Ioan Pop. "Thermal radiation and MHD effects in the mixed convection flow of Fe_3O_4-water ferrofluid towards a nonlinearly moving surface." *Processes* 8, no. 1 (2020): 95. https://doi.org/10.3390/pr8010095

[5] Hosseinzadeh, Kh, So Roghani, A. Asadi, Amirreza Mogharrebi, and D. D. Ganji. "Investigation of micropolar hybrid ferrofluid flow over a vertical plate by considering various base fluid and nanoparticle shape factor." *International*

Journal of Numerical Methods for Heat & Fluid Flow 31, no. 1 (2021): 402-417. https://doi.org/10.1108/HFF-02-2020-0095

[6] Yasin, Siti Hanani Mat, Muhammad Khairul Anuar Mohamed, Zulkhibri Ismail, and Mohd Zuki Salleh. "Mathematical solution on MHD stagnation point flow of ferrofluid." In *Defect and Diffusion Forum*, vol. 399, pp. 38-54. Trans Tech Publications Ltd, 2020. https://doi.org/10.4028/www.scientific.net/DDF.399.38

[7] Tlili, Iskander, M. T. Mustafa, K. Anantha Kumar, and N. Sandeep. "Effect of asymmetrical heat rise/fall on the film flow of magnetohydrodynamic hybrid ferrofluid." *Scientific Reports* 10, no. 1 (2020): 6677. https://doi.org/10.1038/s41598-020-63708-y

[8] Mohamed, Muhammad Khairul Anuar, Siti Hanani Mat Yasin, Mohd Zuki Salleh, and Hamzeh Taha Alkasasbeh. "MHD stagnation point flow and heat transfer over a stretching sheet in a blood-based casson ferrofluid with newtonian heating." *Journal of Advanced Research in Fluid Mechanics and Thermal Sciences* 82, no. 1 (2021): 1-11. https://doi.org/10.37934/arfmts.82.1.111

[9] Rosli, Wan Muhammad Hilmi Wan, Muhammad Khairul Anuar Mohamed, Norhafizah Md Sarif, Nurul Farahain Mohammad, and Siti Khuzaimah Soid. "Boundary layer flow of Williamson hybrid ferrofluid over a permeable stretching sheet with thermal radiation effects." *CFD Letters* 15, no. 3 (2023): 112-122. https://doi.org/10.37934/cfdl.15.3.112122

[10] Abdelsalam, Sara I., and M. M. Bhatti. "New insight into AuNP applications in tumour treatment and cosmetics through wavy annuli at the nanoscale." *Scientific Reports* 9, no. 1 (2019): 260. https://doi.org/10.1038/s41598-018-36459-0

[11] Alam, Jahangir, Ghulam Murtaza, Efstratios Tzirtzilakis, and Mohammad Ferdows. "Biomagnetic fluid flow and heat transfer study of blood with gold nanoparticles over a stretching sheet in the presence of magnetic dipole." *Fluids* 6, no. 3 (2021): 113. https://doi.org/10.3390/fluids6030113

[12] Royal Institution. "Michael Faraday's gold colloids." *The Royal Institution: Science Lives Here*.

[13] Rahbari, A., M. Fakour, A. Hamzehnezhad, M. Akbari Vakilabadi, and D. D. Ganji. "Heat transfer and fluid flow of blood with nanoparticles through porous vessels in a magnetic field: A quasi-one dimensional analytical approach." *Mathematical Biosciences* 283 (2017): 38-47. https://doi.org/10.1016/j.mbs.2016.11.009

[14] Huang, Xiaohua, and Mostafa A. El-Sayed. "Gold nanoparticles: Optical properties and implementations in cancer diagnosis and photothermal therapy." *Journal of Advanced Research* 1, no. 1 (2010): 13-28. https://doi.org/10.1016/j.jare.2010.02.002

[15] Koriko, Olubode K., I. L. Animasaun, B. Mahanthesh, S. Saleem, G. Sarojamma, and R. Sivaraj. "Heat transfer in the flow of blood-gold Carreau nanofluid induced by partial slip and buoyancy." *Heat Transfer-Asian Research* 47, no. 6 (2018): 806-823. https://doi.org/10.1002/htj.21342

[16] Khan, Umair, Aurang Zaib, Anuar Ishak, Sakhinah Abu Bakar, Isaac Lare Animasaun, and Se-Jin Yook. "Insights into the dynamics of blood conveying gold nanoparticles on a curved surface when suction, thermal radiation, and Lorentz force are significant: The case of Non-Newtonian Williamson fluid." *Mathematics and Computers in Simulation* 193 (2022): 250-268. https://doi.org/10.1016/j.matcom.2021.10.014

[17] Rosli, Wan Muhammad Hilmi Wan, Muhammad Khairul Anuar Mohamed, Norhafizah Md Sarif, Nurul Farahain Mohammad, and Siti Khuzaimah Soid. "Blood conveying ferroparticle flow on a stagnation point over a stretching sheet: Non-Newtonian Williamson hybrid ferrofluid." *Journal of Advanced Research in Fluid Mechanics and Thermal Sciences* 97, no. 2 (2022): 175-185. https://doi.org/10.37934/arfmts.97.2.175185

[18] Srivastava, Neetu. "The Casson fluid model for blood flow through an inclined tapered artery of an accelerated body in the presence of magnetic field." *International Journal of Biomedical Engineering and Technology* 15, no. 3 (2014): 198-210. https://doi.org/10.1504/IJBET.2014.064646

[19] Nagarani, P., and G. Sarojamma. "Effect of body acceleration on pulsatile flow of Casson fluid through a mild stenosed artery." *Korea-Australia Rheology Journal* 20, no. 4 (2008): 189-196.

[20] Loganathan, P., and S. Sangeetha. "Effect of Williamson parameter on Cu-water Williamson nanofluid over a vertical plate." *International Communications in Heat and Mass Transfer* 137 (2022): 106273. https://doi.org/10.1016/j.icheatmasstransfer.2022.106273

[21] Maaitah, Hussein, Abdullah N. Olimat, Omar Quran, and Hamzeh M. Duwairi. "Viscous dissipation analysis of Williamson fluid over a horizontal saturated porous plate at constant wall temperature." *International Journal of Thermofluids* 19 (2023): 100361. https://doi.org/10.1016/j.ijft.2023.100361

[22] Shaheen, S., M. B. Arain, Kottakkaran Sooppy Nisar, Ashwag Albakri, M. D. Shamshuddin, and Fouad Othman Mallawi. "A case study of heat transmission in a Williamson fluid flow through a ciliated porous channel: A semi-numerical approach." *Case Studies in Thermal Engineering* 41 (2023): 102523. https://doi.org/10.1016/j.csite.2022.102523

[23] Gaffar, S. Abdul, V. Ramachandra Prasad, and E. Keshava Reddy. "Computational study of Jeffrey's non-Newtonian fluid past a semi-infinite vertical plate with thermal radiation and heat generation/absorption." *Ain Shams Engineering Journal* 8, no. 2 (2017): 277-294. https://doi.org/10.1016/j.asej.2016.09.003

[24] Zehra, Iffat, Malik Muhammad Yousaf, and Sohail Nadeem. "Numerical solutions of Williamson fluid with pressure dependent viscosity." *Results in Physics* 5 (2015): 20-25. https://doi.org/10.1016/j.rinp.2014.12.002

[25] Ramesh, G. K., B. J. Gireesha, and Rama Subba Reddy Gorla. "Study on Sakiadis and Blasius flows of Williamson fluid with convective boundary condition." *Nonlinear Engineering* 4, no. 4 (2015): 215-221. https://doi.org/10.1515/nleng-2015-0020

[26] Kho, Yap Bing, Abid Hussanan, Muhammad Khairul Anuar Mohamed, and Mohd Zuki Salleh. "Heat and mass transfer analysis on flow of Williamson nanofluid with thermal and velocity slips: Buongiorno model." *Propulsion and Power Research* 8, no. 3 (2019): 243-252. https://doi.org/10.1016/j.jppr.2019.01.011

[27] Imran, Mohd, Nasser Zouli, Tansir Ahamad, Saad M. Alshehri, Mohammed Rehaan Chandan, Shahir Hussain, Abdul Aziz, Mushtaq Ahmad Dar, and Afzal Khan. "Carbon-coated Fe_3O_4 core-shell super-paramagnetic nanoparticle-based ferrofluid for heat transfer applications." *Nanoscale Advances* 3, no. 7 (2021): 1962-1975. https://doi.org/10.1039/D1NA00061F

[28] Mohamed, Muhammad Khairul Anuar, Mohd Zuki Salleh, Fadhilah Che Jamil, and Ong Huei. "Free convection boundary layer flow over a horizontal circular cylinder in Al_2O_3-Ag/water hybrid nanofluid with viscous dissipation." *Malaysian Journal of Fundamental and Applied Sciences* 17, no. 1 (2021): 20-25. https://doi.org/10.11113/mjfas.v17n1.1964

[29] Swalmeh, Mohammed Z., Hamzeh T. Alkasasbeh, Abid Hussanan, and Mustafa Mamat. "Heat transfer flow of Cu-water and Al_2O_3-water micropolar nanofluids about a solid sphere in the presence of natural convection using Keller-box method." *Results in Physics* 9 (2018): 717-724. https://doi.org/10.1016/j.rinp.2018.03.033

[30] Devi, Suriya Uma, and S. P. Anjali Devi. "Heat transfer enhancement of Cu−Al_2O_3/water hybrid nanofluid flow over a stretching sheet." *Journal of the Nigerian Mathematical Society* 36, no. 2 (2017): 419-433.

[31] Merkin, John H. "Free convection boundary layer on an isothermal horizontal cylinder." *American Society of Mechanical Engineers and American Institute of Chemical Engineers* (1976).

[32] Molla, Md Mamun, Md Anwar Hossain, and Manosh C. Paul. "Natural convection flow from an isothermal horizontal circular cylinder in presence of heat generation." *International Journal of Engineering Science* 44, no. 13-14 (2006): 949-958. https://doi.org/10.1016/j.ijengsci.2006.05.002